Exclusive vector meson electroproduction at HERA

Aharon Levy
Tel Aviv University and DESY

Abstract

The latest results on exclusive vector meson electroproduction from HERA are reviewed. In particular, the new high-statistics measurements of the ρ^0 electroproduction are presented and compared to several models.

1 Introduction

Exclusive electroproduction of light vector mesons is a particularly good process for studying the transition from the soft to the hard regime of strong interactions, the former being well described within the Regge phenomenology while the latter - by perturbative QCD (pQCD). Among the most striking expectations [1] in this transition is the change of the logarithmic derivative δ of the cross section σ with respect to the $\gamma^* p$ center-of-mass energy W, from a value of about 0.2 in the soft regime (represented by a soft Pomeron [2] exchange diagram in Fig. 1) to 0.8 in the hard one (represented by a two-gluon exchange diagram in Fig. 2), and the decrease of the exponential slope b of the differential cross section with respect to the squared-four-momentum transfer t, from a value of about 10 GeV^{-2} to an asymptotic value of about 5 GeV^{-2} when the virtuality Q^2 of the photon increases.

When calculating the cross section of exclusive electroproduction of vector mesons (V), one needs information on the wave function of the initial virtual photon, the wave function of the produced vector meson, the $q\bar{q}p$ scattering amplitude, which requires the gluon density and the p elastic form factor (see Fig. 2). In the following we present the available data on exclusive vector

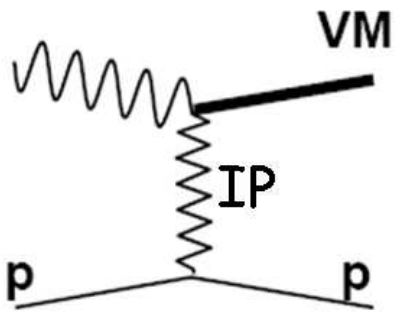

Fig. 1: *A diagram describing exclusive vector meson electroproduction in terms of a Pomeron exchange.*

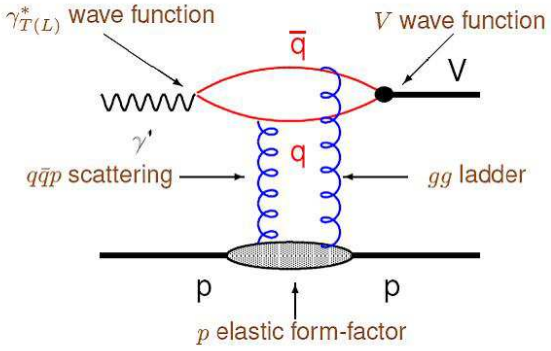

Fig. 2: *A diagram describing exclusive vector meson electroproduction in terms of a two-gluon exchange.*

meson electroproduction and then use the recent precision measurements by ZEUS [3] of the ρ^0 vector meson to discuss what one can learn about the produced vector meson wave function and about the gluon density in the proton.

2 W dependence of the cross section

The soft to hard transition can be seen by studying the W dependence of the cross section for exclusive vector meson photoproduction, from the lightest one, ρ^0, to the heavier ones, up to the Υ. The scale in this case is the mass of the vector meson, as in photoproduction Q^2 = 0. Figure 3 shows $\sigma(\gamma p \rightarrow Vp)$ as function of W for light and heavy vector mesons. For comparison, the total photoproduction cross section, $\sigma_{tot}(\gamma p)$, is also shown. The data at high W can be parameterised as W^δ, and the value of δ is displayed in the figure for each reaction. One sees clearly the transition from a shallow W dependence for low scales to a steeper one as the scale increases.

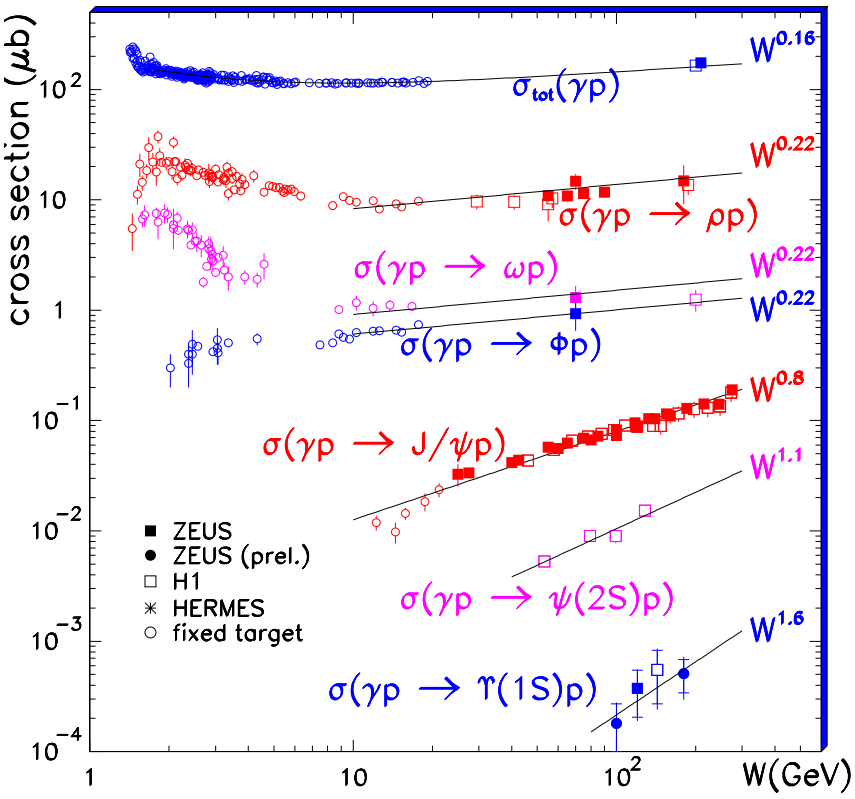

Fig. 3: *The W dependence of the cross section for exclusive vector meson photoproduction, $\sigma(\gamma p \rightarrow Vp)$. The total photoproduction cross section is also shown. The lines are the result of a fit of the form W^δ to the high energy part of the data.*

One can also check this transition by varying Q^2 for a given vector meson. The cross section $\sigma(\gamma^* p \rightarrow \rho^0 p)$ is presented in Fig. 4 as a function of W, for different values of Q^2. The cross section rises with W in all Q^2 bins. In order to quantify this rise, the logarithmic derivative δ of σ with respect to W is obtained by fitting the data to the expression $\sigma \sim W^\delta$ in each of the Q^2 intervals. The resulting values of δ from the recent ZEUS measurement are compiled

in Fig 5. Also included in this figure are values of δ from other measurements [4] for the ρ^0 as well as those for ϕ [5], J/ψ [6] and γ [7] (Deeply Virtual Compton Scattering (DVCS)). In this case the results are plotted as a function of $Q^2 + M^2$, where M is the mass of the vector meson. One sees a universal behaviour, showing an increase of δ as the scale becomes larger, in agreement with the expectations mentioned in the introduction. The value of δ at low scale is the one expected from the soft Pomeron intercept [2], while the one at large scale is in accordance with twice the logarithmic derivative of the gluon density with respect to W.

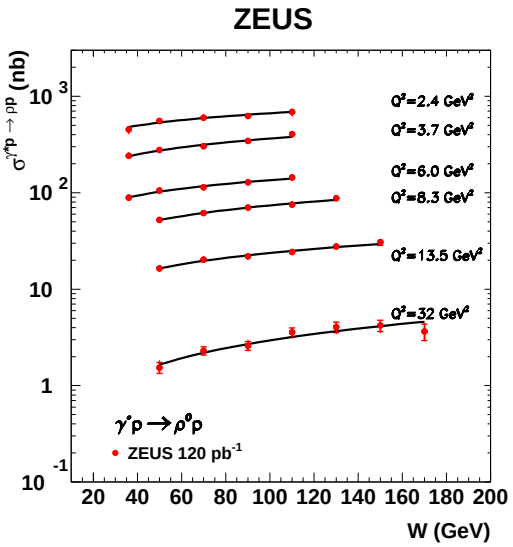

Fig. 4: *The W dependence of the cross section for exclusive ρ^0 electroproduction, for different Q^2 values, as indicated in the figure. The lines are the result of a fit of the form W^δ to the data.*

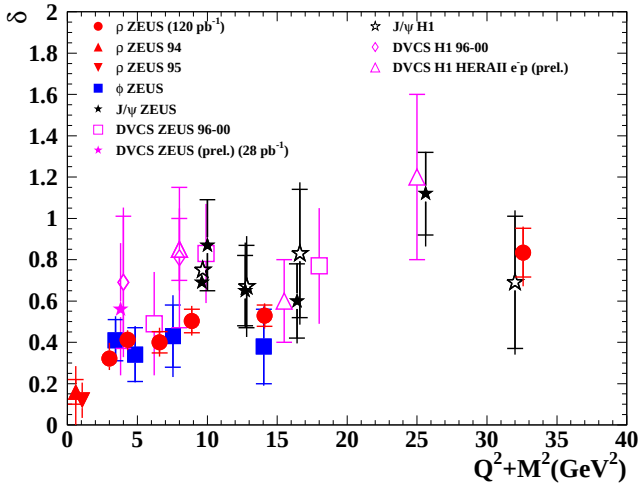

Fig. 5: *A compilation of the value of δ from a fit of the form W^δ for exclusive vector-meson electroproduction, as a function of $Q^2 + M^2$. It includes also the DVCS results.*

3 t dependence of the cross section

The differential cross section, dσ/dt, has been parameterised by an exponential function $e^{-b|t|}$ and fitted to the data of exclusive vector meson electroproduction and also to DVCS. The resulting values of b as a function of the scale $Q^2 + M^2$ are plotted in Fig. 6. As expected, b decreases to a universal value of about 5 GeV^{-2} as the scale increases.

The value of b can be related via a Fourier transform to the impact parameter. Assuming that the process of exclusive electroproduction of vector mesons is hard and dominated by gluons, one can use the relation $< r^2 >= b(\hbar c)^2$ to obtain the radius of the gluon density in the proton. The value of about 5 GeV^{-2} corresponds to a value of $< r >_g \sim$ 0.6 fm, smaller than the value of the charge density of the proton ($< r >_p \sim$ 0.8 fm), indicating that the gluons are well-contained within the charge-radius of the proton.

One can study the W dependence of dσ/dt for fixed t values and extract the effective Pomeron trajectory $\alpha_{IP}(t)$. This was done in case of the ρ^0 for two Q^2 values and the trajectory was fitted to a linear form to obtain the intercept $\alpha_{IP}(0)$ and the slope α'_{IP}. These values are

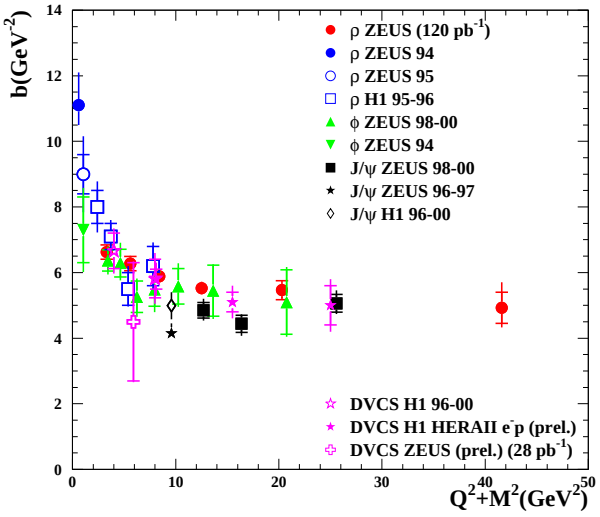

Fig. 6: *A compilation of the value of the slope b from a fit of the form $d\sigma/d|t| \propto e^{-b|t|}$ for exclusive vector-meson electroproduction, as a function of Q^2+M^2. Also included is the DVCS result.*

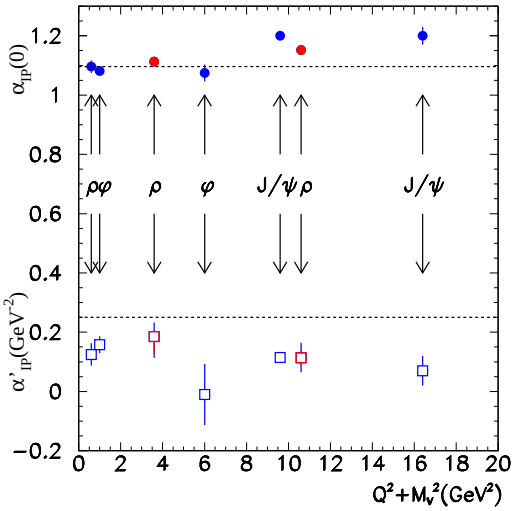

Fig. 7: *Values of the intercept and slope of the effective Pomeron trajectory as a function of Q^2+M^2, as obtained from measurements of exclusive electroproduction of ρ^0, ϕ, and J/ψ vector mesons.*

presented in a compilation of the effective Pomeron intercept and slope, from this and from similar studies for other vector mesons, in Fig. 7. As in the other compilations, the values are plotted as a function of Q^2+M^2. The value of $\alpha_{IP}(0)$ increases with Q^2 while the value of α'_{IP} tends to decrease with Q^2.

4 Q^2, W and t dependence of $r_{00}^{04} = \sigma_L/\sigma_{tot}$ for $\gamma^* p \to \rho^0 p$

The helicity analysis of the decay-matrix element r_{00}^{04} of the ρ^0 was used to extract the ratio $R = \sigma_L/\sigma_T$ of longitudinal (σ_L) to transverse (σ_T) $\gamma^* p$ cross sections. When the value of r_{00}^{04} is close to one, as is the case for this analysis, the error on R becomes large and highly asymmetric. It is then advantageous to study the properties of r_{00}^{04} itself which carries the same information ($= \sigma_L/\sigma_{tot}$), rather than R. While r_{00}^{04} is an increasing function of Q^2, as shown in Fig. 8, it is independent of W in all Q^2 intervals (Fig. 9). This implies that the W behaviour of σ_L is the same as that of σ_T, a result which is somewhat surprising. The $q\bar{q}$ configurations in the wave function of γ_L^* have typically a small transverse size, while the configurations contributing to γ_T^* may have large transverse sizes. The contribution to σ_T of large-size $q\bar{q}$ configurations, which are more hadron-like, is expected to lead to a shallower W dependence than in case of σ_L. Thus, the result presented in Fig. 9 suggests that the large-size configurations of the transversely polarised photon are suppressed.

The above conclusion can also explain the behaviour of r_{00}^{04} as a function of t, shown in Fig. 10 for two Q^2 values. Different sizes of interacting objects imply different t distributions, in particular a steeper $d\sigma_T/dt$ compared to $d\sigma_L/dt$. This turns out not to be the case. In both Q^2

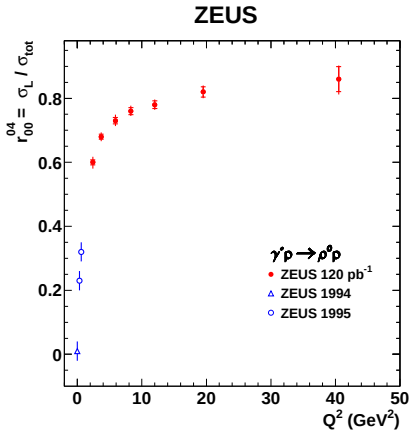

Fig. 8: *The ratio r_{00}^{04} as a function of Q^2 for $W = 90$ GeV.*

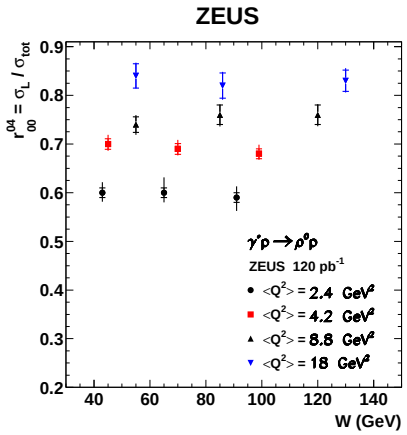

Fig. 9: *The ratio r_{00}^{04} as a function of W for different values of Q^2, as indicated in the figure.*

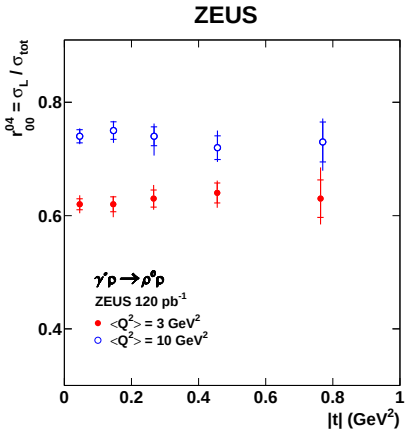

Fig. 10: *The ratio r_{00}^{04} as a function of $|t|$ for different values of Q^2, as indicated in the figure.*

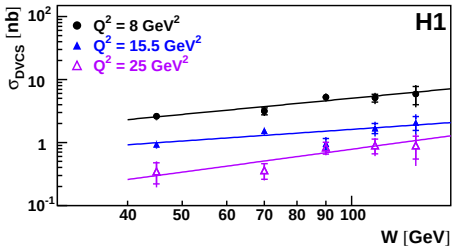

Fig. 11: *The DVCS cross section as a function of W at three values of Q^2. The solid lines represent the results of fits of the form W^δ.*

ranges, r_{00}^{04} is independent of t, reinforcing the earlier conclusion about the suppression of the large-size configurations in the transversely polarised photon.

This suppression is also seen in DVCS, $\gamma^* p \to \gamma p$. The final state photon is real and therefore transversely polarised. Using s-channel helicity conservation, also the initial virtual photon would be transversely polarised. Looking at the new H1 measurement of the DVCS cross section [8], shown in Fig. 11, which has a steep W dependence ($\delta \sim 0.8$), one concludes that the large-size configurations in the transversely polarised photon are suppressed.

5 Comparison of the data of $\gamma^* p \to \rho^0 p$ to models

The precision measurements of the reaction $\gamma^* p \to \rho^0 p$ were used to compare to some selected pQCD-inspired models.

All models are based on the dipole representation of the virtual photon, in which the photon first fluctuates into a $q\bar{q}$ pair (colour dipole), which then interacts with the proton to produce the ρ^0. The ingredients necessary in such calculations are the virtual-photon wave-function, the

dipole-proton cross section and the ρ^0 wave-function. The photon wave-function is known from QED. The models differ in the treatment of the dipole-proton cross section and the assumed ρ^0 wave-function.

The models of Frankfurt, Koepf and Strikman (FKS) [9] and of Martin, Ryskin and Teubner (MRT) [10] are based on two-gluon exchange as the dominant mechanism for the dipole-proton interaction. The gluon distributions are derived from inclusive measurements of the proton structure function. In the FKS model, a three-dimensional Gaussian is assumed for the ρ^0 wave-function, while MRT use parton-hadron duality and normalise the calculations to the data. For the comparison with the present measurements the MRST99 [11] and CTEQ6.5M [12] parameterisations for the gluon density were used.

Kowalski, Motyka and Watt (KMW) [13] use an improved version of the saturation model [14], with an explicit dependence on the impact parameter and DGLAP evolution in Q^2, introduced through the unintegrated gluon distribution [15]. Forshaw, Sandapen and Shaw (FSS) [16] model the dipole-proton interaction through the exchange of a soft [2] and a hard [17] Pomeron, with (Sat) and without (Nosat) saturation, and use the DGKP and Gaussian ρ^0 wave-functions. In the model of Dosch and Ferreira (DF) [18], the dipole cross section is calculated using Wilson loops, making use of the stochastic vacuum model for the non-perturbative QCD contribution.

While the calculations based on two-gluon exchange are limited to relatively high-Q^2 values (typically ~ 4 GeV^2), those based on modelling the dipole cross section incorporate both the perturbative and non-perturbative aspects of ρ^0 production.

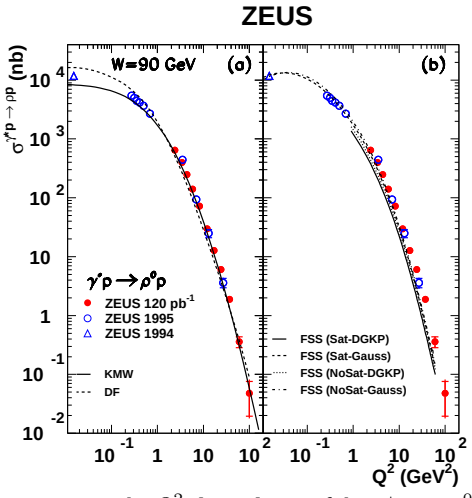

Fig. 12: *The Q^2 dependence of the $\gamma^* p \to \rho^0 p$ cross section at W=90 GeV. The same data are plotted in (a) and (b), compared to different models, as described in the text.*

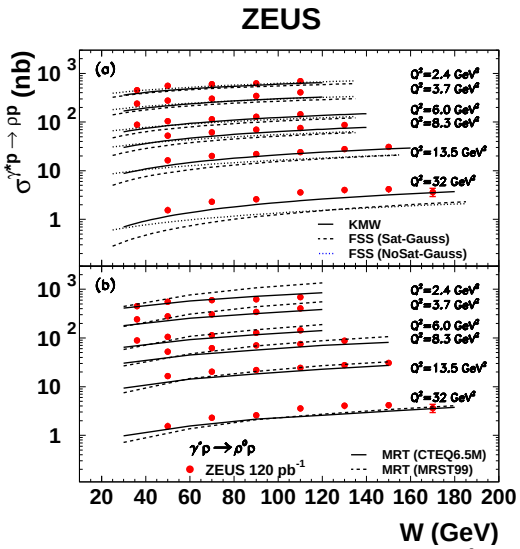

Fig. 13: *The W dependence of the $\gamma^* p \to \rho^0 p$ cross section for different values of Q^2, as indicated in the figure. The same data are plotted in (a) and (b), compared to different models, as described in the text.*

The different predictions discussed above are compared to the Q^2 dependence of the cross section in Fig. 12. None of the models gives a good description of the data over the full kine-

matic range of the measurement. The FSS model with the three-dimensional Gaussian ρ^0 wave-function describes the low-Q^2 data very well, while the KMW and DF models describe the $Q^2 > 1$ GeV^2 region well.

The various predictions are also compared with the W dependence of the cross section, for different Q^2 values, in Fig. 13. Here again, none of the models reproduces the magnitude of the cross section measurements. The closest to the data, in shape and magnitude, are the MRT model with the CTEQ6.5M parametrisation of the gluon distribution in the proton and the KMW model.

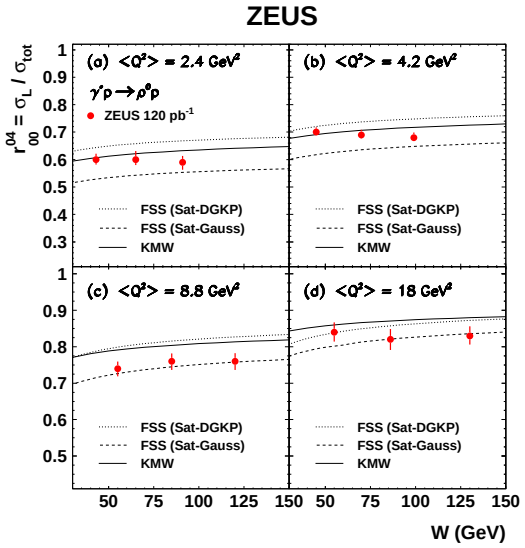

Fig. 14: *The ratio r_{00}^{04} as a function of W for different values of Q^2 compared to the predictions of models as indicated in the figure (see text).*

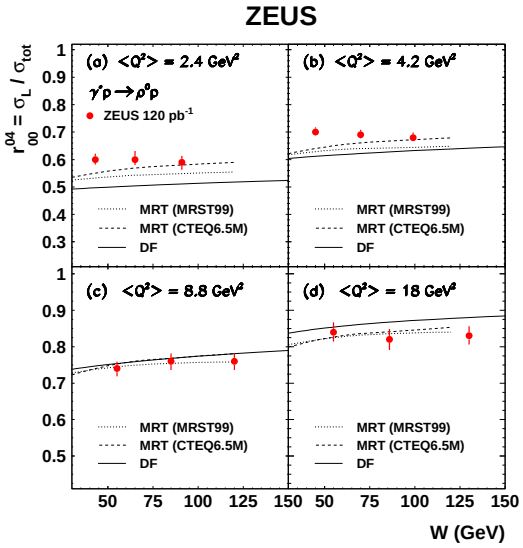

Fig. 15: *The ratio r_{00}^{04} as a function of W for different values of Q^2 compared to the predictions of models as indicated in the figure (see text).*

While all the models exhibit a mild dependence of r_{00}^{04} on W, consistent with the data as shown in Figs. 14 and 15, none of them reproduces correctly the magnitude of r_{00}^{04} in all the Q^2 bins.

In summary, none of the models considered above is able to describe all the features of the data. The high precision of the measurements can be used to refine models for exclusive ρ^0 electroproduction and contribute to a better understanding of the ρ^0 wave function and of the gluon density in the proton.

References

[1] H. Abramowicz, L. Frankfurt and M. Strikman, *Interplay of hard and soft physics in small x deep inelastic processes*, Surveys High Energy Phys. **11**, 51 (1997).

[2] A. Donnachie and P.V. Landshoff, *Total cross-sections*, Phys. Lett. **B 296**, 227 (1992).

[3] ZEUS Coll., S. Chekanov et al., *Exclusive ρ^0 production in deep inelastic scattering at HERA*, DESY07-118 (2007).

[4] ZEUS Coll., J. Breitweg et al., *Elastic and Proton-Dissociative ρ^0 Photoproduction at HERA*, Eur. Phys. J. **C 2**, 2 (1998); ZEUS Coll., M. Derrick et al., *Exclusive Electroproduction of ρ^0 and J/ψ Mesons at HERA*, Eur. Phys. J. **C 6**, 603 (1999); H1 Coll., C. Adloff et al., *Elastic electroproduction of ρ mesons at HERA*, Eur. Phys. J. **C 13**, 371 (2000).

[5] H1 Coll., C. Adloff et al., *Measurement of elastic electroproduction of ϕ mesons at HERA*, Phys. Lett. **B 483**, 360 (2000); ZEUS Coll., S. Chekanov et al., *Exclusive Electroproduction of ϕ Mesons at HERA*, Nucl. Phys. **B 718**, 3 (2005).

[6] ZEUS Coll., S. Chekanov et al. *Exclusive electroproduction of J/ψ mesons at HERA*, Nucl. Phys. **B 695**, 3 (2004); H1 Coll., A. Aktas et al., *Elastic J/ψ production at HERA*, Eur. Phys. J. **C 46**, 585 (2006).

[7] ZEUS Coll., S. Chekanov et al., *Measurement of deeply virtual Compton scattering at HERA*, Phys. Lett. **B 573**, 46 (2003); H1 Coll., A. Aktas et al., *Measurement of Deeply Virtual Compton scattering at HERA*, Eur. Phys. J. **C 44**, 1 (2005).

[8] H1 Coll., A. Aktas et al., *Measurement of Deeply Virtual Compton scattering and its t-dependence at HERA*, DESY-07-142 (2007).

[9] L. Frankfurt, W. Koepf and M. Strikman, *Diffractive heavy quarkonium photoproduction and electroproduction in QCD*, Phys. Rev. **D 57**, 512 (1998); L. Frankfurt, W. Koepf and M. Strikman, *Hard diffractive electroproduction of vector mesons in QCD*, Phys. Rev. **D 54**, 3194 (1996).

[10] A.D. Martin, M.G. Ryskin and T. Teubner, *Q^2 dependence of diffractive vector meson electroproduction*, Phys. Rev. **D 62**, 014022 (2000).

[11] A.D. Martin, R.G. Roberts, W.J. Stirling and R.S. Thorne, *Parton distributions: A New global analysis*, Eur. Phys. J. **C 4**, 463 (1998).

[12] W.K. Tung, H.L. Lai, A. Belyaev, J. Pumplin, D. Stump and C.-P. Yuan, *Heavy Quark Mass Effects in Deep Inelastic Scattering and Global QCD Analysis*, JHEP **0702**, 053 (2007),

[13] H. Kowalski, L. Motyka and G. Watt, *Exclusive diffractive processes at HERA within the dipole picture*, Phys. Rev. **D 74**, 074016 (2006).

[14] K. Golec-Biernat and M. Wuesthoff, *Saturation effects in deep inelastic scattering at low Q^2 and its implications on diffraction*, Phys. Rev. **D 59**, 014017 (1999); K. Golec-Biernat and M. Wuesthoff, *Saturation in diffractive deep inelastic scattering*, Phys. Rev. **D 60**, 114023 (1999).

[15] See e.g. M.A. Kimber, A.D. Martin and M.G. Ryskin, *Unintegrated parton distributions*, Phys. Rev. **D63**, 114027 (2001).

[16] J.R. Forshaw, R. Sandapen and G. Shaw, *Color dipoles and ρ, ϕ electroproduction*, Phys. Rev **D 69**, 094013 (2004).

[17] A. Donnachie and P.V. Landshoff, *New data and the hard Pomeron*, Phys. Lett. **B 518**, 63 (2001).

[18] H.G. Dosch and E. Ferreira, *Nonperturbative and perturbative aspects of photo- and electroproduction of vector mesons*, hep-ph/0610311 (2006).